Kovacs effect and fluctuation–dissipation relations in 1D kinetically constrained models

2003 J. Phys. A: Math. Gen. 36 12367

(http://iopscience.iop.org/0305-4470/36/50/002)

INSTITUTE OF PHYSICS PUBLISHING JOURNAL OF PHYSICS A: MATHEMATICAL AND GENERAL

J. Phys. A: Math. Gen. **36** (2003) 12367–12377 PII: S0305-4470(03)67107-6

Kovacs effect and fluctuation–dissipation relations in 1D kinetically constrained models

Arnaud Buhot

UMR 5819 (CNRS, CEA, UJF), SI3M/DRFMC, CEA Grenoble, 17 rue des Martyrs, 38054 Grenoble cedex 9, France

E-mail: abuhot@cea.fr.

Received 1 August 2003, in final form 3 September 2003
Published 2 December 2003
Online at stacks.iop.org/JPhysA/36/12367

Abstract

Strong and fragile glass relaxation behaviours are obtained simply changing the constraints of the kinetically constrained Ising chain from symmetric to purely asymmetric. We study the out-of-equilibrium dynamics of these two models focusing on the Kovacs effect and the fluctuation–dissipation (FD) relations. The Kovacs or memory effect, commonly observed in structural glasses, is present for both constraints but enhanced with the asymmetric ones. Most surprisingly, the related FD relations satisfy the FD theorem in both cases. This result strongly differs from the simple quenching procedure where the asymmetric model presents strong deviations from the FD theorem.

PACS numbers: 75.10.Pq, 05.70.Ln, 75.40.Mg

1. Introduction

The Kovacs or memory effect has been observed by Kovacs himself in the 1960s on structural glassy systems [1]. It is a surprising memory effect of the energy (or volume) of the system following a particular quenching procedure. This quenching procedure consists in suddenly cooling a glassy system from a high temperature (infinite one in our case) to a very low intermediate temperature T_i and letting the system relax. When the waiting time t_w necessary for the energy of the system to reach the equilibrium value for a final temperature T_f is attained ($e(t_w) = e_{\mathrm{eq}}(T_f)$), the temperature of the system is set to this value $T_f \geqslant T_i$. The result found by Kovacs is that, even though the system is at the equilibrium energy (the volume in his case) corresponding to the temperature imposed, the system and its energy are still evolving. The system keeps memory of its history and of the fact that equilibrium is not effective. After a rapid increase of the energy, the system reaches the equilibrium and the energy decreases and levels off that equilibrium leading to a hump in the energy as a function of time.

In this paper, we are interested in a comparison of the Kovacs effect for two simple (even simplistic) models with respectively strong and fragile glass behaviours. We consider the

symmetric and purely asymmetric kinetically constrained Ising chain (KCIC) models [2, 3]. This simple change of the kinetic constraints allows one to switch respectively from strong to fragile glass behaviour. The underlying equilibrium being the same for both models, a direct comparison of the dynamical effects is possible.

After a short presentation of the models in section 2, the Kovacs effect is discussed in section 3. The effect is observed in both models considered but is enhanced in the asymmetric case. This section also contains simple rescaling arguments to explain this effect and a comparison with recent works on the Kovacs effect [4–7]. The fluctuation–dissipation (FD) relations are studied during the Kovacs quenching procedure and presented in section 4. The FD relations satisfy the FD theorem in both cases. These results are in strong contradiction with those obtained using a simple quenching procedure from high temperature to a low final temperature after a waiting time t_w. This last quenching procedure leads to FD relations satisfying the FD theorem for the symmetric KCIC model and for waiting times well below the relaxation time. In contrast, strong deviations from the FD theorem have been observed for the asymmetric KCIC model for waiting times smaller than the equilibration time. We give some conclusions in section 5.

2. Presentation of the models

In this paper, we are interested in the possible difference concerning the Kovacs effect due to strong or fragile glass behaviour. We thus consider the KCIC model [2, 3] for which constraints may be chosen to model strong (for symmetric ones) and fragile (for a purely asymmetric chain) glass relaxations.

Let us consider a chain of N Ising spins ($\sigma_i = 0, 1$ with $i = 1, \ldots, N$) without interactions where spins $\sigma_i = 1$ are considered as defects. The corresponding Hamiltonian is thus trivial ($H = \sum_i \sigma_i$) as well as the equilibrium thermodynamic properties. The equilibrium energy at temperature T or inverse temperature β is given by $e_{\mathrm{eq}}(T = 1/\beta) = 1/(1 + \mathrm{e}^{\beta})$ which is also the concentration of defects or the probability to have a defect at site i. It is possible to determine exactly the probability for a defect to have its next defect (on the left) at a distance d

$$P_{\mathrm{eq}}(d, T) = e_{\mathrm{eq}}(1 - e_{\mathrm{eq}})^{d-1}. \tag{1}$$

The first term on the right-hand side of the equation corresponds to the probability to have a defect whereas the second term (with a power $d - 1$) is the probability to have no defects in the intermediate $d - 1$ sites. The non-interacting spins render at equilibrium the probabilities at each sites independent of each other and lead to this simple product in $P_{\mathrm{eq}}(d, T)$.

All these equilibrium properties are independent of any dynamics considered. However, the introduction of kinetic constraints allows one to obtain a slowing down of the dynamics characteristic of glassy systems before the equilibrium properties are reached. The probability for a spin to flip is constrained in the following way: in the symmetric case, a spin is able to flip as soon as a neighbour (left or right) is a defect whereas, in the asymmetric case, the defect has to be on the left. Such spins are also called spin facilitated and their probability transitions are given by the following equation:

$$P(\sigma_i \to 1 - \sigma_i) = \min(1, \mathrm{e}^{\beta(2\sigma_i - 1)})(b\sigma_{i-1} + (1 - b)\sigma_{i+1}). \tag{2}$$

The first term on the right-hand side corresponds to the usual Metropolis probability and allows one to satisfy the detailed balance. The second term corresponds to the general kinetic constraints with a probability b to flip the spin if there is a left neighbour and $1 - b$ for a right neighbour. The symmetric model ($b = 1/2$) and the purely asymmetric one ($b = 0$ or 1) correspond to particular values of this parameter b.

These models have been extensively studied (for more information and references on kinetically constrained models see the recent review by Ritort and Sollich [8]). With the symmetric constraints, the dynamical behaviour is reminiscent of a strong glass with a relaxation time following an Arrhenius law. At sufficiently low temperature, the defects are mainly isolated and may be considered as simple particles diffusing with a temperature-dependent rate of diffusion $\Gamma \sim \exp(-1/T)$. The energy (or concentration of particles) evolves through creation and annihilation processes. Similar reaction-diffusion models have been introduced for a long time to study domain growth, coarsening and ageing [9–11]. Within the asymmetric constraints, the energy barriers involved in the motion of defects are increasing logarithmically with the distance from the next defect [12]. As a consequence, the relaxation time follows the Bässler law [13]: $t_{\rm relax} \sim \exp(1/T^2 \ln 2)$. Whereas the Arrhenius behaviour is associated to a strong glass behaviour following the Angell's classification [14], the super-Arrhenius behaviour of the asymmetric model is associated to a fragile glass. Intermediate constraints allow the system to continuously crossover from fragile to strong glass behaviour [15] but will not be considered in this study.

3. Kovacs effect

As already mentioned in the introduction, the Kovacs effect is observed following a particular quenching procedure. At time $t = 0$, a system, equilibrated at high temperature ($T = \infty$ in our case), is suddenly quenched to an intermediate low temperature T_i. The system starts to relax and the energy decreases until it reaches the equilibrium energy corresponding to a final temperature $T_f \geqslant T_i$ after a waiting time $t_w(T_i, T_f)$ defined by the following equation:

$$e(t_w) = \frac{1}{N}\sum_i \sigma_i(t_w) = e_{\rm eq}(T_f) = (1 + {\rm e}^{\beta_f})^{-1} \tag{3}$$

where $e(t)$ is the energy of the system at time t and $\beta = 1/T$ is the inverse temperature. The temperature of the system is set to T_f at this waiting time t_w.

If the system was characterized only by the thermodynamical parameters (energy, volume and temperature), we would expect the energy of the system to stay constant and equal to $e_{\rm eq}(T_f)$ after the waiting time t_w. However, even though its energy corresponds to that equilibrium one at the imposed temperature, the particular configuration of the system at t_w is still far from an equilibrium configuration at T_f. As a consequence, the energy is still evolving after t_w.

3.1. The symmetric KCIC model

Figure 1 illustrates the Kovacs effect for the symmetric KCIC model[1]. As can be seen on the left panel, the Kovacs effect is an increasing function of the difference between the intermediate and final temperatures. A two timescale behaviour is also clearly observed. The energy increases on a timescale $t \sim O(1)$ to reach a plateau followed by a further increase up to a maximum. The energy finally decreases to reach the equilibrium energy at temperature T_f. Note also that the maximum in energy decreases and shifts to slightly higher times for higher intermediate temperatures T_i. This result was already observed for the volume by Kovacs [1] and for the energy in recent simulations [4, 5].

[1] Numerical simulations have been done using the continuous time algorithm [16] on systems of size $N = 10^6$ and averaged on 20–50 runs. For the FD relations, the strength of the field $h = 0.05$ was sufficient to be in the linear regime.

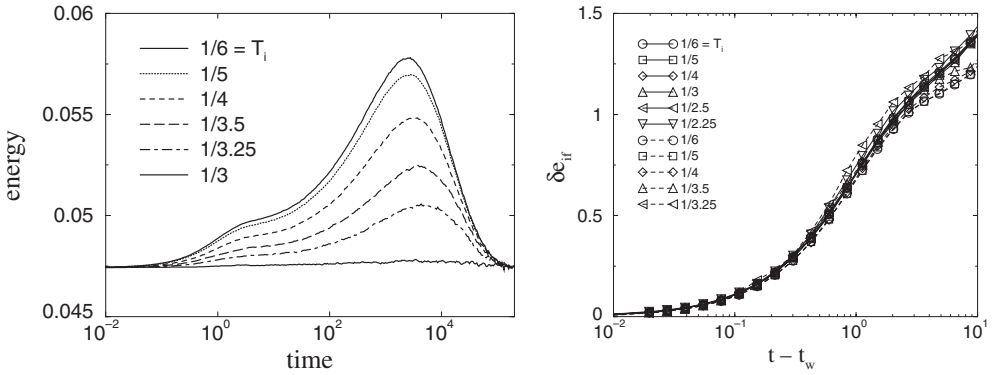

Figure 1. Left : Kovacs effect for a final temperature $T_f = 1/3$ and different intermediate temperatures T_i within the symmetric KCIC model: the energy as a function of time elapsed since the waiting time is plotted. Right: the rescaled energy δe_{if} for short times (see text for definition) is plotted for two final temperatures $T_f = 1/2$ (full lines) and $1/3$ (dashed lines) and for different intermediate temperatures.

The maximum of the energy is obtained for a timescale $t_m \sim O(\exp(3/T_f))$. This timescale is of the same order as the equilibrium timescale $t_{\rm eq}$ (time to reach the equilibrium after a rapid quench from a high temperature to a low temperature T_f) [3, 8]. This $\exp(3/T_f)$ dependence of $t_{\rm eq}$ is explained considering that the energy $e(t)$ after such a quench decays like the annihilation process $A + A \rightarrow A$ in one dimension with a diffusion rate Γ: $e(t) \sim (\Gamma t)^{-1/2}$. The energy thus reaches that equilibrium ($e_{\rm eq}(T_f) \sim {\rm e}^{-1/T_f}$) after an equilibrium time $t_{\rm eq} \sim \Gamma^{-1} e_{\rm eq}^{-2} \sim e^{3/T_f}$ due to the temperature-dependent diffusion rate ($\Gamma \sim {\rm e}^{-1/T_f}$). With a similar argument it is possible to estimate the waiting time $t_w(T_i, T_f) \sim \Gamma^{-1}(T_i) e_{\rm eq}^{-2}(T_f) \sim {\rm e}^{1/T_i}\,{\rm e}^{2/T_f}$ where the equilibrium energy to reach is $e_{\rm eq}(T_f) \sim {\rm e}^{-1/T_f}$ but the diffusion rate is $\Gamma(T_i) \sim {\rm e}^{-1/T_i}$ since the temperature of the system before t_w is set to T_i. We recover the equilibrium time when $T_i = T_f$. The estimate of the waiting time agrees qualitatively with the values obtained from numerical simulations for the different couples of intermediate and final temperatures considered.

Let us now analyse the short timescales behaviour. The fast increase of the energy is related to the probability p_i to have neighbouring defects. Such a probability is given at t_w by $p_i = e(t_w) e_{\rm eq}(T_i)$ where $e(t_w) = e_{\rm eq}(T_f)$ is the probability to have a defect at t_w and $e_{\rm eq}(T_i)$ is the probability for its neighbour to also be a defect. This last term corresponds to the equilibrium probability $P_{\rm eq}(d = 1, T_i)$ due to the fact that the timescale to equilibrate the concentration of neighbouring defects (or non-constrained defects) is $t \sim O(1) \ll t_w$ and has thus already equilibrated at t_w. When the temperature is increased from the low temperature T_i to a higher one T_f, on a similar timescale $t - t_w \sim O(1)$ independent of the temperature, the probability to have neighbouring defects reaches its equilibrium value $p_f = e_{\rm eq}^2(T_f)$. Furthermore, the timescale for the motion of defects is $\Gamma^{-1}(T_f) \sim \exp(1/T_f) \gg 1$. As a consequence, the change of probability from p_i to p_f is mainly obtained from the creation of defects and the energy as a function of time may be expressed as

$$e(t - t_w) = e_{\rm eq} + (p_f - p_i)\delta e_{if}(t - t_w) \tag{4}$$

where we expect $\delta e_{if}(t - t_w)$ to be independent of both intermediate and final temperatures for $t - t_w \sim O(1)$ and to start to differ at $\delta e_{if} \simeq 1$ for different T_f. This prediction is verified in the right panel of figure 1 where δe_{if} is plotted for different couples (T_i, T_f) on short times $t - t_w$.

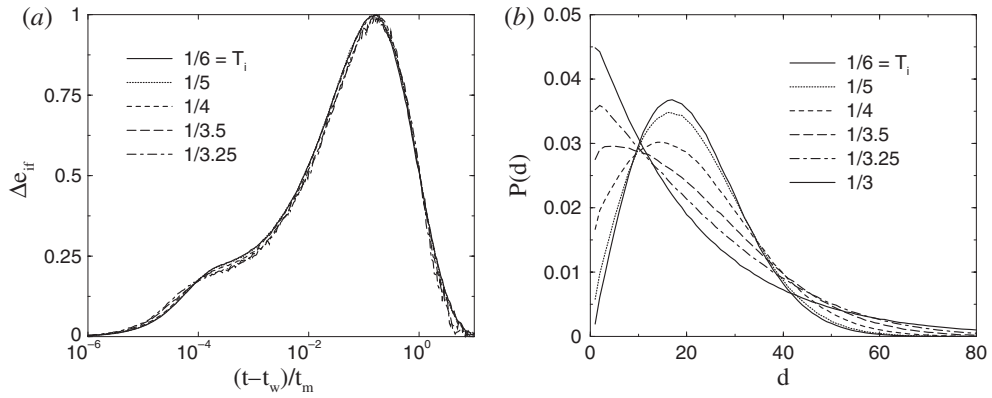

Figure 2. (*a*) Rescaled energy Δe_{if} as a function of the rescaled time $(t - t_w)/t_m$ (see text for definition) and (*b*) the distribution of distances between defects at the different waiting times $t_w(T_i, T_f)$. For both figures, the model considered is the symmetric KCIC and the final temperature is $T_f = 1/3$.

On longer timescales, the activated regime is involved. The defects may then be considered as simple particles moving with a temperature-dependent diffusion rate $\Gamma_f \sim \exp(-1/T_f)$. The number of particles (or energy) evolves through creation of neighbouring defects and annihilation when two defects collide ($A + A \leftrightarrow A$). As we have seen with the short timescales behaviour, the energy increases after the waiting time t_w. This increase is not restricted to the short timescales but continues on longer timescales and is due to the fact that the distribution of distances between defects $P(d)$ at the different waiting times $t_w(T_i, T_f)$ is far from the equilibrium one $P_{\rm eq}(d, T_f)$ (see equation (2) for definition). This difference is evident in the right panel of figure 2. The distribution $P(d)$ converges to that equilibrium when the intermediate temperature reaches the final one as it should. One important point is that the whole range of the distribution is affected. Defects with neighbouring defects at all distances relax with the same typical timescale due to the single energy barrier involved (the motion of a defect from one site to the next one is independent of the distance from its neighbouring defect).

The interpretation with diffusive particles and with annihilation–creation processes is similar to coarsening models. The only differences with the 1D Ising model concern the diffusive rate which is temperature-dependent in our case and the creation–annihilation processes which are of the type $A + A \leftrightarrow \emptyset$ in the Ising model. This analogy to domain growth models allows us to use the same rescaling for long timescales of the Kovacs effect. In recent works [4–6], it has been shown that, for domain growth models, the energy shift from the equilibrium energy may be rescaled for all intermediate temperatures T_i in the following way:

$$e(t) = e_{\rm eq}(T_f) + e_m \Delta e_{if} \left(\frac{t - t_w}{t_m} \right) \tag{5}$$

where t_m is the time for which the shift in energy from the equilibrium energy already diminished by a factor two from its maximum value

$$e(t_m) = e_{\rm eq}(T_f) + e_m/2. \tag{6}$$

As can be seen in the left panel of figure 2, this rescaling is correct for the long timescales. For short timescales, a small deviation from this rescaling is observed.

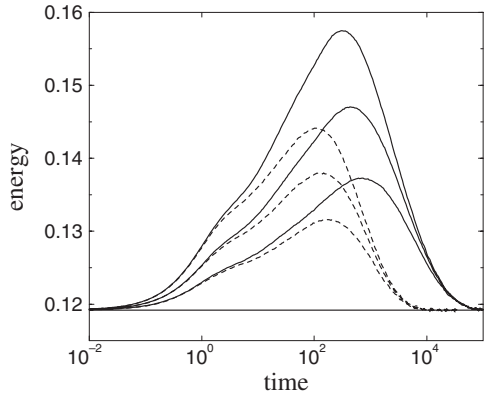

Figure 3. Comparison of the Kovacs effect for the symmetric (dashed lines) and the asymmetric (full lines) KCIC models. The energy as a function of time elapsed since the waiting time is plotted for a final temperature $T_f = 1/2$ and different intermediate temperatures $T_i = 1/4$, $1/3$ and $1/2.5$.

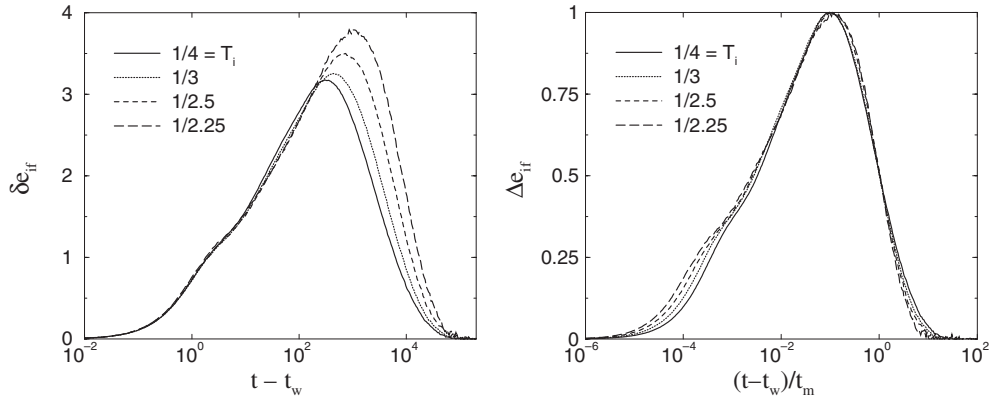

Figure 4. Kovacs effect for the final temperature $T_f = 1/2$ and different intermediate temperatures T_i with the asymmetric KCIC model. On the left figure are plotted the rescaled energy δe_{if} for short timescales as a function of time since the waiting time and, on the right figure, the rescaled energy for long timescales as a function of the rescaled time.

3.2. The asymmetric KCIC model and comparison

In figure 3, we compare the Kovacs effects for the symmetric and asymmetric KCIC models. The energy as a function of the time $t - t_w$ since the final temperature $T_f = 1/2$ was set to the system is plotted for different intermediate temperatures $T_i = 1/4$, $1/3$ and $1/2.5$. As can be seen, the short timescales behaviour (non-activated) is similar in both models. The same rescaling introduced for the symmetric KCIC model works perfectly on short timescales for the asymmetric KCIC model (see left panel of figure 4). The argument developed to obtain the rescaling is independent of the dynamical constraints as soon as the motion of particles occurs on timescales larger than the spontaneous creation of neighbouring defects.

On longer timescales, when activation plays an important role, the Kovacs effect starts to differ between the symmetric and asymmetric KCIC models. The main result is a higher maximum of the energy for the asymmetric case. The timescales involved are also not surprisingly different due to equilibration times which strongly differ from strong to fragile

glass behaviour. This can also be traced out on the values of the waiting times $t_w(T_i, T_f)$ larger for the asymmetric KCIC model (fragile glass behaviour) than for the symmetric KCIC model (strong glass behaviour). From the analysis of Sollich and Evans [12], it is possible to have an estimate of the waiting time $t_w(T_i, T_f)$ for the asymmetric KCIC model. The same creation–annihilation processes occur as for the symmetric KCIC model but the motion of particles may not be considered as simple diffusion due to the increasing energy barriers with the distance between defects. An anomalous coarsening occurs where the energy decreases like $e(t) \sim t^{-T_i \ln 2}$ with a temperature-dependent exponent in contrast to normal coarsening. The waiting time is obtained when the energy reaches the equilibrium energy $e_{\rm eq}(T_f) \sim {\rm e}^{-1/T_f}$ leading to $t_w(T_i, T_f) \sim \exp(1/T_i T_f \ln 2)$. Note that once again we recover the equilibrium timescale $t_{\rm eq}(T_f) \sim \exp\left(1/T_f^2 \ln 2\right)$ when $T_i = T_f$. The estimate for the waiting time agrees qualitatively with the values obtained from the numerical simulations for different couples of intermediate and final temperatures.

We use the rescaling for the long timescales of coarsening models (5) (see right panel of figure 4) as for the symmetric KCIC model. We observe some deviations from a perfect rescaling even for the long timescales. This difference is due to the anomalous coarsening behaviour of the asymmetric KCIC model. The failure of the rescaling on short timescales is also more evident.

4. Fluctuation–dissipation relations

The violation of the fluctuation–dissipation (FD) theorem is usually present in glassy systems due to the out-of-equilibrium dynamics (see for example the recent review by Crisanti and Ritort [17] and the references therein). FD relations have already been considered for the symmetric and asymmetric KCIC models in [18] with the usual quenching procedure. A more careful analysis of the symmetric case leads to the conclusion that even far from equilibrium (at least after a short transient), the FD relations satisfy the FD theorem for all temperatures and waiting times [19]. This result was explained by the fact that defects are mainly isolated at low temperatures after a short transient and behave as in local equilibrium (with a temperature-dependent diffusive rate $\Gamma \sim \exp(-1/T)$) even if the number of defects is larger than in equilibrium. This argument is no longer valid for the asymmetric case where the motion of a defect is dependent on the position of its left neighbour defect and is thus sensitive to the total number of defects or at least to the distribution of distances between defects which is out-of-equilibrium. The differences between the FD relations for both models are evident in figure 5 following the usual quenching procedure. We consider such FD relations after the Kovacs quenching procedure to check if this discrepancy between the two models is also present.

Let us first explain how these FD relations are determined. The integrated response is determined following the now standard procedure introduced by Barrat [20]. A pertubation $\delta H(t) = -h(t) \sum_i \varepsilon_i \sigma_i$ is added to the Hamiltonian where $h(t) = h\Theta(t - t_w)$ is a field of strength h introduced after the waiting time t_w ($\Theta(x)$ is the Heaviside function). Random fields are set to each site through the random variables $\varepsilon_i = \pm 1$ with identical probabilities. The integrated response is then

$$\chi(t, t_w) = \frac{1}{hN} \sum_i \overline{\varepsilon_i \langle \sigma_i(t) \rangle_h} \tag{7}$$

with the overline standing for an average over the random variables ε_i and the brackets for the dynamical average in the presence of the perturbation. Note that in these kinetically constrained models different dynamics may be considered after the introduction of the perturbation. We

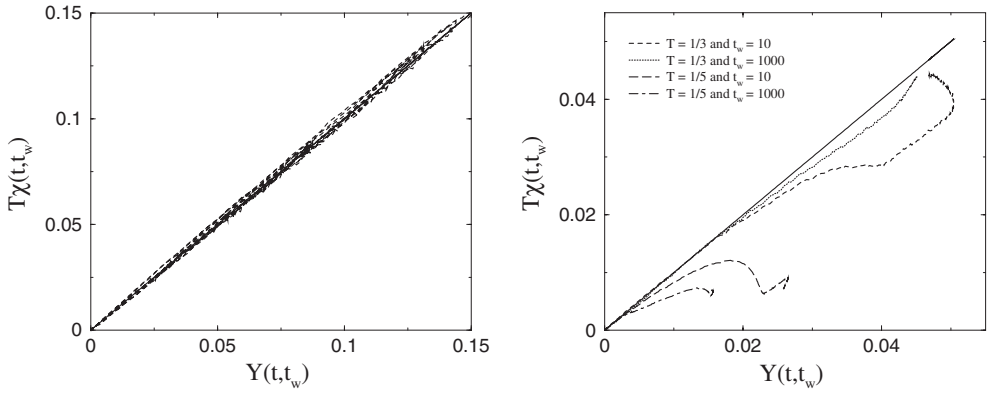

Figure 5. Fluctuation–dissipation relations for the symmetric (left) and asymmetric (right) KCIC models with a usual quenching procedure (see text for explanation). A set of final temperatures ($T_f = 1/\beta_f = 1/3$ and $1/6$) and waiting times ($t_w = 10$, 100, 1000 and 10 000) have been studied and all couples of temperatures-waiting times (dotted lines) satisfy the FD theorem (full line) in the symmetric case. A set of final temperatures ($T_f = 1/\beta_f = 3$ and 5) and waiting times ($t_w = 10$ and 1000) have been studied and strong deviation from the FD theorem (full line) have been observed for all couples of temperatures-waiting times in the asymmetric case.

considered the modified Metropolis one discussed in [21] which gives similar results to the Metropolis one in this case (see footnote 1).

The integrated response has to be compared to the corresponding correlations to check the validity of the FD theorem. In the case where the energy is still evolving the correct correlations to consider are the connected ones

$$C(t, t_w) = \frac{1}{N} \sum_i \langle \sigma_i(t) \sigma_i(t_w) \rangle - e(t) e(t_w) \tag{8}$$

where $e(t)$ is the energy at time t and the brackets stand for the dynamical average without the perturbation. In equilibrium, the integrated response and correlations only depend on the difference of times and satisfy: $T\chi(t - t_w) = C(0) - C(t - t_w)$. It has been shown in [19] that a correct generalization of this expression for systems out-of-equilibrium is

$$T\chi(t, t_w) = f(Y(t, t_w)) \tag{9}$$

with $Y(t, t_w) \equiv C(t, t) - C(t, t_w)$. If the FD theorem is satisfied the function $f(x) = x$. Thus, a parametric plot of the integrated response with respect to the function Y allows one to check the validity of the FD theorem. Note that in these kinetically constrained systems, $C(t, t) = e(t) - e^2(t)$ depends on time. This explains the parametric plot with respect to $Y(t, t_w)$ instead of the two-time correlation $C(t, t_w)$. A slope X different than 1 in this parametric plot would suggest the existence of an effective temperature $T_{\text{eff}} = T/X$.

In figure 5, we have plotted the FD relations for both symmetric (left) and asymmetric (right) KCIC models following the usual quenching procedure. At $t = 0$, the system is quenched from an infinite temperature to a low temperature T_f. The perturbation is introduced at a waiting time t_w after this quench. On the left panel, the FD relations for the symmetric KCIC model satisfy the FD theorem for a large set of temperatures and waiting times (as soon as $t_w > 1$). The validity of the FD theorem is far from obvious if we keep in mind that both the integrated response and $Y(t, t_w)$ are non-monotonic. However, they compensate each other to follow the FD theorem curve at all times. The non-monotonic behaviour of the response is due to the decrease of the energy on long timescales. When rescaled by the energy, the response is continuously increasing.

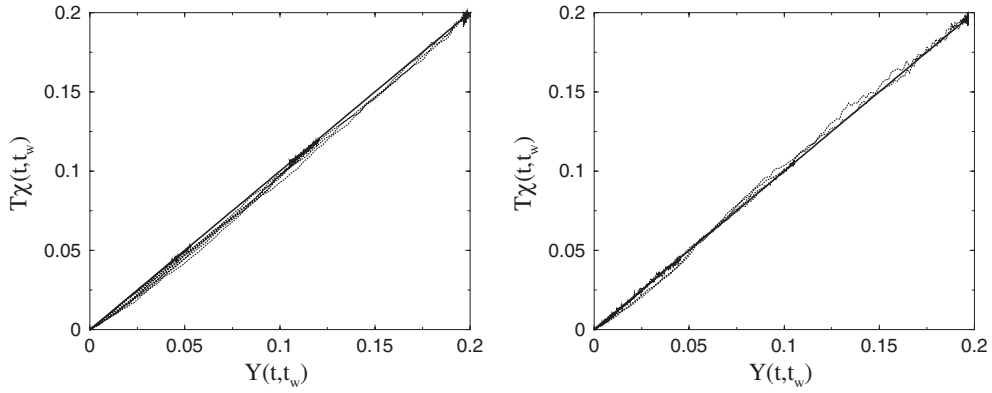

Figure 6. Fluctuation–dissipation relation for the symmetric (left) and asymmetric (right) KCIC models with a Kovacs quenching procedure (see text for explanation). A set of intermediate and final temperatures ($T_i = 1/\beta_i$, $T_f = 1/\beta_f$) have been studied and all couples of temperatures (dotted lines) satisfy the FD theorem (full line). Final and intermediate inverse temperatures considered for the symmetric case: $\beta_f = 1$, 2 and 3 and $\beta_i = 3$, 4 and 5 and for the asymmetric case: $\beta_f = 1$, 2 and 3 and $\beta_i = 3$ and 4.

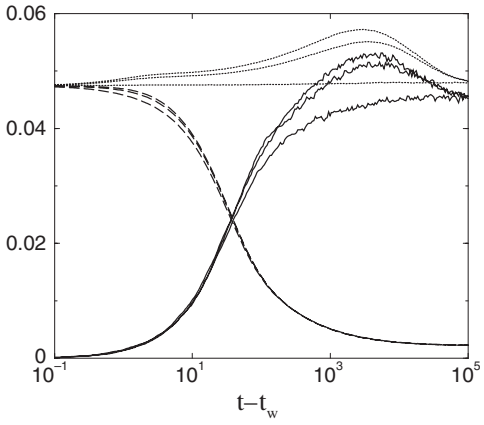

Figure 7. Responses (full lines), energies (dotted lines) and correlations (dashed lines) for different intermediate temperatures T_i (from top to bottom $T_i = 1/5$, $1/4$ and $1/3$) for the symmetric KCIC model with $T_f = 1/3$.

For the asymmetric KCIC model, the FD relations show strong deviation from the FD theorem. The non-monotonic integrated response cannot be accounted for by the difference of correlations $Y(t, t_w)$ as it is for the symmetric KCIC model. It leads to different humps in the FD relations corresponding to the different plateaus observed in the decay of the energy. The increasing energy barriers ($\Delta E = 1, 2, \ldots$) lead to those different plateaus in the energy decay after a quench in temperature [12, 15]. The FD theorem is recovered for sufficiently large waiting times (for $t_w > 10^4$ when $T_f = 1/3$ for example).

Let us now consider the FD relations for the symmetric (left) and asymmetric (right) KCIC models after the Kovacs quenching procedure (see figure 6). As can be seen in both cases the FD theorem is verified. This is in strong contrast with the evolution of the energy which shows a deviation from equilibrium. This deviation is sufficiently important to exclude the fact that it does not show up on the FD relations. In figure 7 we can observe that the

responses for different intermediate temperatures as well as the energies and the correlations are different. However, the FD theorem is satisfied. Note for example that when T_i is much lower than T_f, the response shows a hump which may be related directly to the fact that the energy is not constant. An increasing energy, corresponding to a larger number of defects, tends to increase the response. The further decrease of the response is then related to the same decrease in the energy. The consequence on the FD relations is that the parametric curve increases from the origin to a maximum before a small decrease occurs but always following the line $f(x) = x$ corresponding to the FD theorem curve.

The fact that the FD relations follow the FD theorem curve for the symmetric KCIC model is not surprising since it is already the case after a usual quenching procedure. A simple explanation suggesting that defects are in local equilibrium has been given. The surprise comes from the asymmetric KCIC model where the FD relations differ strongly from the FD theorem curve for most waiting times with the usual quenching procedure. With the Kovacs one, the FD relations follow the FD theorem curve. A possible argument would be the following. The waiting times involved in the Kovacs quenching procedure are sufficiently large that the out-of-equilibrium configuration may be considered as equivalent to a simple fluctuation in the system at equilibrium. In other words the linear regime is attained and the FD theorem is satisfied. However, this argument would not explain the shift in energy observed.

5. Conclusion

In this paper, we have studied the Kovacs effect for the symmetric and asymmetric KCIC models with respectively strong and fragile glass behaviours. The effect is stronger in the asymmetric case. The symmetric KCIC model satisfies the same rescaling as domain growth models for long timescales. Some small deviations are present for the asymmetric KCIC model and may be explained due to the anomalous coarsening. The short timescales behaviour is identical for both models and a simple argument allows one to rescale all simulations for different intermediate and final temperatures on the same leading curve which happens to be independent of the dynamics (identical for the symmetric and asymmetric KCIC models).

We have also studied the FD relations for both models after a Kovacs quenching and a usual one. After the Kovacs quenching, the related FD relations verify surprisingly the FD theorem for both models in strong contrast with the results for the asymmetric KCIC model using the usual quenching procedure. No clear explanation has been found for this behaviour. It could be interesting to have a look at the Kovacs effect and the corresponding FD relations using the models introduced in [21] where analytical results may be expected due to the possible exact mean-field solution.

Acknowledgments

The author would like to thank R Calemczuk for useful discussions and a careful reading of the manuscript.

References

[1] Kovacs A J 1963 *Fortscher. Hochpolym. Forsch. (Adv. Polym. Sci.)* **3** 394
Kovacs A J, Aklonis J J, Hutchinson J M and Ramos A R 1979 *J. Polym. Sci.* **17** 1097–162
[2] Fredrickson G H and Andersen H C 1984 *Phys. Rev. Lett.* **53** 1244–7
[3] Jäckle J and Eisinger S 1991 *Z. Phys.* B **84** 115
[4] Berthier L and Holdsworth P C W 2002 *Europhys. Lett.* **58** 35–42

[5] Berthier L and Bouchaud J P 2002 *Phys. Rev.* B **66** 054404
[6] Bertin E M, Bouchaud J P, Drouffe J M and Godrèche C 2003 *Preprint* cond-mat/0306089
[7] Mossa S and Sciortino F 2003 *Preprint* cond-mat/0305526
[8] Ritort F and Sollich P 2003 *Adv. Phys.* **52** 219–342
[9] Burschka M A, Doering C R and ben-Avraham D 1989 *Phys. Rev. Lett.* **63** 700–3
[10] Masser T O and ben-Avraham D 2001 *Phys. Rev.* E **63** 066108
[11] Yuste S B and Lindenberg K 2001 *Phys. Rev. Lett.* **87** 118301
[12] Sollich P and Evans M R 1999 *Phys. Rev. Lett.* **83** 3238–41
Sollich P and Evans M R 2003 *Phys. Rev.* E **68** 031504
[13] Bässler H 1987 *Phys. Rev. Lett.* **58** 767–70
[14] Angell C A 1995 *Science* **267** 1924–35
[15] Buhot A and Garrahan J P 2001 *Phys. Rev.* E **64** 021505
Buhot A and Garrahan J P 2002 *J. Phys.: Condens. Matter* **14** 1499–507
[16] Bortz A B, Kalos M H and Lebowitz J L 1975 *J. Comput. Phys.* **17** 10
Newman M E J and Barkema G T 1999 *Monte-Carlo Methods in Statistical Physics* (Oxford: Oxford University Press)
[17] Crisanti A and Ritort F 2003 *J. Phys. A: Math. Gen.* **36** R181–R290
[18] Crisanti A, Ritort F, Rocco A and Sellitto M 2000 *J. Chem. Phys.* **113** 10615–34
[19] Buhot A and Garrahan J P 2002 *Phys. Rev. Lett.* **88** 225702
[20] Barrat A 1998 *Phys. Rev.* E **57** 3629–32
[21] Buhot A, Garrahan J P and Sherrington D 2003 *J. Phys. A: Math. Gen.* **36** 307–28